Designing High-Strength Copper Alloys Based on the Crystallographic Structure of Precipitates

by Hidemichi Fujiwara *

ABSTRACT We have developed a technique for advancing the design of precipitation hardened copper alloys using calculations to extract, from a crystallographic data base, those elements and compounds capable of acting as the precipitate phase, and we have verified experimentally the results of those calculations. We have found that in those alloys in which the compounds that were identified by calculation as those in which precipitation would occur during the aging process, precipitation did occur on the habit plane that was predicted by calculation, and precipitation hardening behavior was clearly exhibited. By also taking account of considerations of solid mechanics it has been possible to predict strength after aging, raising the expectation of integrating precipitate (i.e., the alloy system) selection with design for after-aging strength.

1. INTRODUCTION

In recent years precipitation-hardened copper alloys have come into use in applications requiring high-strength electrical conductors, creating an active movement for the development of new alloys. One of the most obvious needs is for high-strength copper alloys, and a large number of precipitation-hardened alloys have been developed [1].

In the conventional approach to alloy development, an alloy system was generally identified on the basis of the temperature dependence of the solid solution limit of the precipitate component, as obtained from a phase diagram for the alloy, and alloy composition was established by evaluating its properties experimentally. At the present time it is rare for alloy design to focus on the parameters that determine alloy strength, i.e., the crystallographic structure of the precipitate phase and the precipitation state itself.

What is more, the actual identification of an alloy using an experimental approach would, in the case of ternary alloy systems, involve upwards of 2400 combinations. When we also consider methods of optimizing the composition, identifying the optimum alloy becomes a practical impossibility.

We accordingly propose, as a means of identifying new alloy systems from among the huge number of existing alloy system combinations, to focus on the crystallographic structure of the precipitate phase, which contributes to precipitation hardening, and are working to identify those alloys that could exist as a precipitation hardened phase, and to predict the conditions of existence of the precipitate phase and the precipitation hardenability [2].

We believe that the method proposed here makes it possible to design alloys by bench-top investigation, using crystallographic structures that form a hardened phase together with a combination of phase diagrams and calculations capable of predicting its volume fraction.

In the following we discuss the methodology used, together with the analytical results obtained.

2. EXPERIMENTAL AND ANALYTICAL METHODOLOGY

2.1 Calculation Method for Predicting the Conditions of Existence of Precipitates in a Matrix

The state of precipitates in a matrix may be characterized with reference to precipitate phase size, distribution density, and the conditions at the interface between the precipitate and matrix phases. Since precipitate size and distribution density are determined by the concentration of the alloy components and the aging conditions, the most important parameter in identifying an alloy system for alloy design is the conditions at the interface between the precipitate and matrix phases, so that the focus must be on the habit plane between the precipitate and the matrix.

Among the conditions for calculating the habit plane, the matching of the atomic alignment period at the interface between the precipitate and the matrix is a necessary condition but when one extends the discussion to interface stability it becomes necessary to take into account the conditions of atomic bonding--that is to say, the magnitude of chemical interfacial energy and the strain energy caused by misfit between the matrix and precipitate phases.

However, in order to keep the interfacial energy value

* Ecology and Energy Lab., R&D Div.

low, a minimal match of the atomic alignment periods is a necessary condition. Therefore in selecting compounds for which a habit plane can exist between the precipitate and matrix phases, we may say the necessary condition is satisfied by matching atomic alignments.

Turning our attention next to the crystallographic structure on the compound side, and considering the symmetricality of the copper crystals that form the matrix, we find ourselves limited to those crystallographic systems having comparatively high symmetry: 1) cubic; 2) tetragonal; 3) orthorhombic; and 4) hexagonal. Since we consider that matching can be easily obtained in these systems we select from these four crystallographic systems those compounds in which a precipitation-hardened phase can occur.

2.1.1 Cubic Crystals

Considering precipitates in cubic systems, they are of the same crystallographic system as the matrix, so that the orientation relationship between the fundamental planes of the two may be said to be:

$(001)_{Cu}//(001)_{p.t.}$, $[100]_{Cu}//[100]_{p.t.}$

In this case two things are necessary:

1) that the fundamental structure of the precipitate be a face-centered structure; and
2) that the lattice constant of the precipitate be close to an integer multiple of that of the matrix (misfit is less than 4 %).

We may express this as

$$a_{p.t.} = \{a_{Cu}\ (1 + \delta)\} \cdot n \qquad (1)$$

where: $a_{p.t.}$ is the lattice constant of the precipitate; a_{Cu} is the lattice constant of the copper matrix; and n is any integer

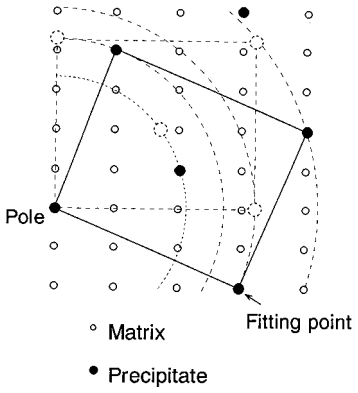

Figure 1 Schematic of the method used to establish the habit plane. (atomic positions of the matrix and precipitate are shown by blank and solid circles respectively)

2.1.2 Tetragonal and Orthorhombic Crystals

To find the habit plane it is necessary to establish two directional vectors of the matrix within that plane, and this involves calculating the fit at the unit vectors for the spacing between the fundamental plane of the precipitate and the azimuthal vectors included within the interface of the matrix side. Figure 1 is a schematic representation of the method. Following is a detailed description of the calculating procedure:

(1) It is essential that at least one lattice constant of the chemical compound be close to an integer multiple of a certain plane spacing of the matrix (misfit less than 4 %), and that a directional vector perpendicular to the plane satisfying this condition and one lattice axis of the compound be the rotational pole. At this point one of the matrix-side vectors included in the habit plane is established.

(2) If, when a unit cell of the compound is rotated about an axis (e.g., the a axis of the compound), the origin of which is one of the atoms located on the matrix plane, the other lattice points of the compound (e.g., atomic points on the b or c axis) match or are extremely close to atomic points on the low-index plane of the matrix (i.e., misfit is less than 4 %), the planes formed by two axes of the above-mentioned compound become the habit planes of the matrix and precipitate respectively, and the orientation relationship can be established.

In terms of the specific method of calculation, it is first necessary to establish the rotational axis of the matrix. In such a case there are few bonding defects in the interface at the low-index plane, so that in terms of interfacial energy it is stable. There are an infinite number of matrix directional vectors for the rotational axis, but if zero is included among the indices, there will of necessity be low-index vectors in the perpendicular direction. These, therefore, must be the basis of our discussion here.

If the relationships described above be represented with reference to rotational axes [001] and [011], we have the following:

I) Considering a rotational axis [001] perpendicular to the (001) plane:

the directional vectors may be represented by the relationship

$[a\ b\ 0] = (n_1[0.5\ 0.5\ 0] + n_2[0.5\ -0.5\ 0]$

where $n_1 + n_2$ must be an even number;

the atomic spacing may be calculated by

$$d_{cu} = d_{100}\ \{1/2\ (n_1^2 + n_2^2)\}^{1/2} \qquad (2)$$

the fitting conditions may be represented by

$$a_{p.t.} = d_{Cu}\ (1 + \delta) \cdot n \qquad (3)$$

and the plane index for the predicted plane will be (b a 0).

II) Considering a rotational axis [011] perpendicular to the (011) plane:

the directional vectors may be represented by the relationship

$[a\ b\ b] = (n_1[1\ 0\ 0] + n_2[0\ 0.5\ 0.5]$

where n_1 must be an integer and n_2 must be an even number;

the atomic spacing may be calculated by

$$d_{Cu} = d_{100}\ \{(n_1^2 + 1/2n_2^2)\}^{1/2} \qquad (4)$$

the fitting conditions may be represented by

$$a_{p.t.} = d_{Cu}\,(1 + \delta) \cdot n \qquad (5)$$

and the plane index for the predicted plane will be (2b a a).

By means of the two relationships described above, it is possible to identify phases having a relationship matching the matrix planes indexed by the relationships (b a 0) and (2b a a).

Further, as stated above, it is also possible to extrapolate the above relationships for higher-index planes, but since the atomic plane density that could make a habit plane would be lower, we confined the analysis presented in this paper to two directional vectors.

2.1.3 Hexagonal Crystals

In the case of a hexagonal crystallographic system, the azimuthal relationship, considered in terms of the atomic surface layer period, would be $(111)_{Cu}//(0001)_{hex}$, and a condition of partial matching can be obtained in cases in which the (110) plane spacing in the matrix (0.256 nm for copper) and the length of the a and b axes of the compound are close to the same.

The fitting conditions are represented by

$$a_{p.t.} = \{a_{Cu}/2\ [110]\ (1 + \delta)\} \cdot n \qquad (6)$$

2.2 Analyzing for Precipitation Hardenability from State of Precipitation

When the precipitate is minutely dispersed and has not reached the over-aging stage, precipitation hardening most often consists of strengthening due to the elastic strain caused by precipitation. The crystallographic structure of the precipitate differs from that of the matrix, and when the interface between the precipitate and matrix phases is coherent, the precipitate forms a coherent dislocation loop and passes through the precipitate without shearing, and in the case of a cubic system that is matched with the precipitate, is thought to be sheared due to dislocation. In either case it is thought that the strengthening due to the elastic strain existing between the matrix and precipitate phases is what determines the degree of precipitation hardening. Using the equations evaluated by Gerold and Haberkom [3], this degree of precipitation hardening may be represented as

$$\Delta\tau \propto |\ \varepsilon\ |^{3/2}\ (f \cdot r)^{1/2} \qquad (7)$$

where: ε is the degree of misfit; f is the volume fraction of precipitate; and r is precipitate radius.

With reference to the relationship between the habit plane and the slip plane, priority should be given to adopting a slip system having a directional vector such that the angle formed between the direction perpendicular to the habit plane at which the precipitate size factor is minimized and the slip plane is the smallest.

As for the precipitate volume fraction f, if we let $\delta\rho$ be the change in resistivity during the aging process and δC be the change in solute concentration in the matrix due to precipitation, which may be found using, inter alia, Linde's Rule [4], we find that $\delta C \propto \delta\rho$, and considering the above-mentioned conditions we may represent the degree of precipitation hardening by

$$\Delta\tau \propto |\ \varepsilon\ |^{3/2}\ \{\delta C \cdot r_a\ (a/b)\}^{1/2}/\sin\theta \qquad (8)$$

where: a is the minimum length of the precipitate phase; b is the maximum length of the precipitate phase; and r_a is the average precipitate diameter; and where θ is the angle formed by the habit plane and the slip plane; and the slip system having the maximum value for $\sin\theta$ is used.

The precipitation hardenability per unit of precipitate can then be found by the partial differential equation

$$\partial\Delta\tau/\partial C \propto |\ \varepsilon\ |^{3/2} \cdot \delta C^{-1/2} \cdot \{r_a\ (a/b)\}^{1/2}/\sin\theta \qquad (9)$$

On the other hand it is thought that the change in hardness δH due to age hardening, as found experimentally, is proportional to $\Delta\tau$, and that the value of $\delta H/\delta C$, obtained by dividing the change in hardness δH by the change in solute concentration δC contributing to precipitation, found from the change in the value for resistivity, is proportional to $\partial\Delta\tau/\partial C$ in Equation (9), so that it becomes possible to compare the calculated and experimental values for the degree of precipitation hardening and the precipitation hardenability.

3. RESULTS AND DISCUSSION

3.1 Results of Compound Selection Based on Fitting Calculations

As a database for compound selection we performed fitting calculations with reference to compounds in the cubic, tetragonal, orthorhombic and hexagonal crystallographic systems contained in Peason's Handbook [5].

Table 1 Results calculated for crystal lattice fitting using data on chemical compounds in Peason's Handbook.

Cubic	Tetragonal	Orthorhombic	Hexagonal
101	16	107	12

As shown in Table 1, the compounds selected comprise 101 of the cubic crystallographic system, 16 of the tetragonal, 107 of the orthorhombic and 12 of the hexagonal, and it may be considered that when compounds were present as a precipitate, there was a habit plane between it and the matrix. It is worthy of note that this occurred more frequently in tetragonal and orthorhombic systems.

Table 2 Results calculated for habit plane selected from data shown in Table 1. (shading shows data that match fitting conditions)

Alloy	Precip.	Crystal sys.	a axis (nm)	b axis (nm)	c axis (nm)	Rot. Pole	Fitting	Habit P.
CuNiTi	Ni_3Ti	Hex.	0.5019	0.5019	0.8299	<111>	(110)	(111)
CuTiSi	CuTiSi	0rtho.	0.6193	3.746	0.713	<100>	(100)	(100)
	TiSi	0rtho.	0.6544	0.3638	0.499	<100>	(110)	(110)
CuCoSi	Co_2Si	0rtho.	0.408	0.373	0.7097	<100>	(110, 100)	(110, 100)
CuCoP	Co_2P	0rtho.	0.565	0.3508	0.6604	<100>	(130)	(130)
CuNiSi	Ni_2Si	0rtho.	0.5	0.372	0.706	<100>	(110, 100)	(110, 100)
CuNiMnP	NiMnP	0rtho.	0.595	0.3557	0.6828	<100>	(130)	(130)
	$NiMn_3P_2$	0rtho.	0.5949	0.3486	0.6865	<100>	(130)	(130)
CuNiAl	Ni_3Al	Cubic	0.357	0.357	0.357	<100>	(100)	(100)

Striped area's data matched to fitting condition.

Table 2 shows a single result selected from the calculated results referred to above. Depending on the compound there are cases in which a plurality of habit plane were selected by calculation, but since, as was described above, interface stability changes in accordance with the atomic bonding condition at the habit plane interface, interfaces with lower interfacial energy were the ones selected [1].

3.2 Comparison Between Habit Plane According to Calculation and Experimental Habit Plane

In order to check the match between the habit plane obtained by calculation and the actual habit plane, comparisons are being performed with the aged phases of actual alloys for the alloy systems shown in Table 2.

Figure 2 shows typical high-resolution observations made using a JEOL JEM3010 transmission electron microscope at 300 kV with reference to Cu-Ti-Si, Cu-Ni-Si, Cu-Ni-Mn-P alloy systems, in which orthorhombic precipitates might be expected to occur. The observations were made after aging at temperatures from 723 to 773 K for from 2 to 24 hr. Since the predicted habit plane index was {0 k l}, we calculated the angles formed between the predicted habit plane and the (010) and (001) planes using an electron beam impingement direction of [100]Cu, and those compared with the high-resolution images observed are also shown. The calculated plane angle and the angle between the (010) plane and the habit plane in the high-resolution images showed good agreement, demonstrating that the precipitation concentration was in accordance with the predictive calculations. Good agreement with the predicted results has been obtained for all of the cubic, hexagonal and orthorhombic crystallographic systems [2]. The agreement of atomic alignment on the habit plane is, as noted in Section 2.1, a necessary condition for structuring the habit plane, and are thought to be useful as conditions for selecting compounds.

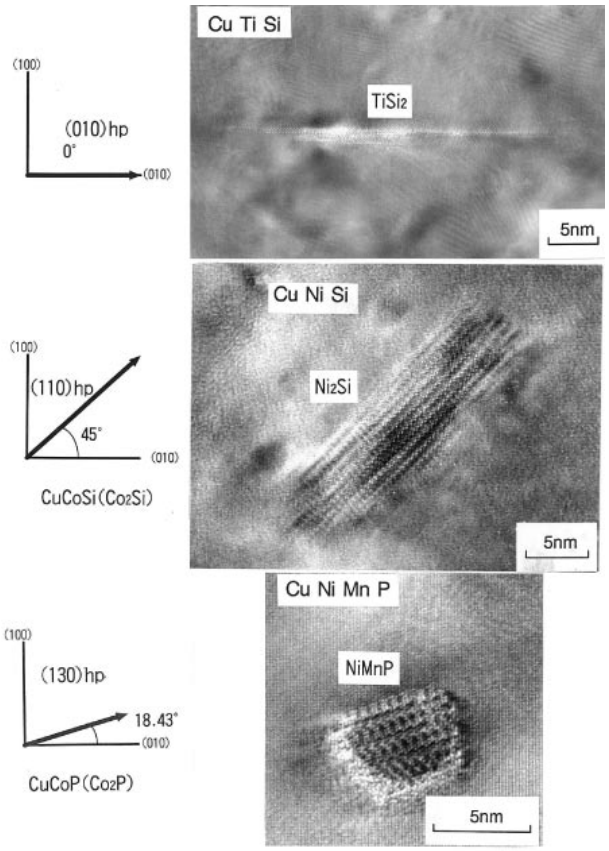

Figure 2 High-resolution TEM images of orthorhombic system precipitates in selected alloys after aging.

3.3 Evaluation of Precipitation Hardenability of Selected Compounds using Calculation and Experiment

In evaluating precipitation hardenability by means of Equation (9) in Section 2.2, we carried out an analysis of precipitation hardenability $\delta H/\delta C$ obtained from aging experiments with reference to the contribution of the various parameters in Equation (9), among which we may mention: a) the change in solute concentration: δC; b) the boundary misfit between matrix and precipitate: ε; c) the precipitate morphology factor: a/b; and d) the angle between the habit plane and the slip plane in the system that moves most easily: θ.

a) Change in solute concentration: δC
b) Boundary misfit between matrix and precipitate: ε
c) Precipitate morphology factor: a/b
d) Angle between slip plane and habit plane: θ

Let it be noted that precipitate size is not considered because, as shown in Table 3, the spherical equivalent diameter of precipitates in the condition where maximum hardness had been reached were virtually identical, irrespective of the alloy system.

Table 3 Experimental results for selected specimens from Table 2 after aging.

Alloy	Crystal system	Experimental habit plane	Aging condition	Hardness change δH	Solute change δC	Precipitate diameter/ mm	Morphology factor a/b
CuNiTi	Hex.	(111)	723K-5h	96.6	2.3806	6.2	0.075
CuTiSi	Ortho.	(100)	773K-5h	54.6	1.5064	7.2	0.013
CuCoSi	Ortho.	(110)	748K-5h	149	2.4142	5.8	0.273
CuCoP	Ortho.	(130)	723K-2h	89.3	0.387	5.2	0.875
CuNiSi	Ortho.	(110)	773K-2h	130	2.4055	6.2	0.288
CuNiMnP	Ortho.	(130)	723K-2h	85	0.9227	5.6	0.72
CuNiAl	Cubic	(100)	723K-5h	23.1	0.5821	5.8	0.5

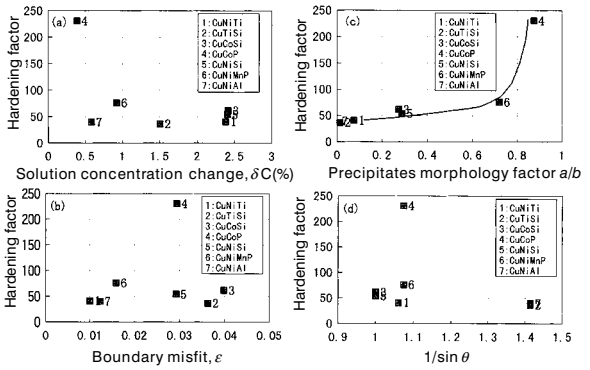

Figure 3 Effect of various parameters in Equation (9) on the precipitation hardening factor.

Figure 3 shows the relationship between precipitation hardenability $\delta H/\delta C$ and the various parameters. The highest correlation was between experimental $\delta H/\delta C$ and precipitate morphology factor a/b, and it can also be seen that a/b is large, i.e., the closer it is to granular the greater the precipitation hardenability.

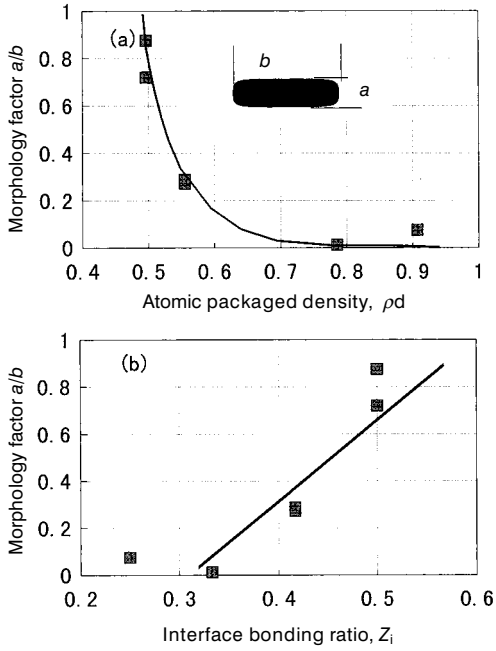

Figure 4 Effect of atomic arrangement parameters on precipitate morphology factor.

As can be seen from Figure 4, the precipitate morphology factor has a correlation with the atomic density of the matrix in the precipitation plane--i.e., the lower the atomic density in the precipitation plane the greater the morphology factor--indicating a tendency to granularity. If this relationship is plotted against Z_i which is the bonding number at the interface with respect to atomic bonding number of matrix (fcc is 12), a substantially linear relationship is obtained.

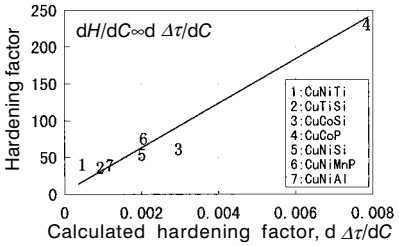

Figure 5 Relationship between experimental and calculated values for precipitation hardening factor.

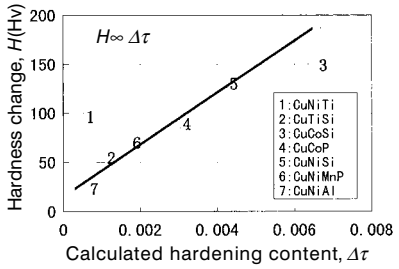

Figure 6 Relationship between experimental and calculated values for parameters of precipitation hardness change.

Figure 5 shows the results of a comparison between experimental values for precipitation hardenability and calculated values for the parameters, and Figure 6 shows the results of a comparison between experimental values for the degree of precipitation hardening and calculated values for a parameter that is proportional to the degree of precipitation hardening. For both precipitation hardenability and degree of precipitation hardening, a good correlation can be observed between the calculated and experimental values, suggesting the validity of the prediction of degree of precipitation hardening using Equation (8) and the evaluation of precipitation hardenability using Equation (9).

In the case of the Ni_3Ti phase, which is a hexagonal system, there is a slight deviation from the distribution of calculated and experimental values shown in Figures 5 and 6 for each of the precipitates. As a cause for this, it may be that, unlike in the precipitate phases of an orthorhombic system, there may be fewer bonding defects on the atomic alignment on the habit line, so that different precipitation hardening mechanisms, such as ordered strengthening may be at work, and it is possible that comparisons with reference to precipitation hardenability must be carried out within hexagonal crystallographic systems.

To summarize the foregoing discussion, when it is considered that as an equation for predicting precipitation hardening parameter from crystallographic data, the precipitate morphology parameter a/b at the habit line and the atomic bonding ratio Z_i are in a substantially linear relationship, we may derive

$$\partial\Delta\tau/\partial C \propto |\varepsilon|^{3/2} \cdot \delta C^{-1/2} \cdot Z_i^{1/2}/\sin\theta \qquad (10)$$

The relationship in Equation (10) shows that if for the habit plane, θ, Z_i and ε are determined based on the calculated results about habit plane, precipitation hardenability $\partial\Delta\tau/\partial C$ can be found by calculation based on the amount of alloy elements.

3.4 Factors Establishing the Habit Plane of Precipitate and Matrix

As we may see from the calculated results shown in Table 2, cases may exist in which a plurality of habit planes may be inferred for a single precipitate. This indicates that it is not possible to fully characterize the habit planes merely with reference to atomic alignment alone. Here, as a method for characterizing habit planes from calculated results, let us proceed with reference to interfacial energy. Interfacial energy understood in the broad sense may be represented as

$$\sigma = \sigma_c + \sigma_e \qquad (11)$$

where: σ_c is chemical energy and σ_e is elastic strain energy, and σ_c may be represented in accordance with Servi and Turnbull [7] by

$$\sigma_c = E_0 N_S Z_S (C - C_a)^2/N_0 Z_L \qquad (12)$$

where: N_s is the number of atoms per unit of interface area; Z_L is the number contributing to bonding (12 for fcc); Z_S is the number of bonds per atom passing through the interface, which is smaller for planes with a higher atomic density of the matrix; E_0 is a value equivalent to the amount of increase of energy due to the average atomic bonds of different kinds; N_0 is the Avogadro number; C is the solute concentration in the precipitate; and C_a is the solute concentration in the matrix.

Provided different kind of atom bonding energy is not negative, the larger the number of atomic bonding defects at the interface the larger E_0 will be and the higher the interfacial energy itself, so that habit plane instability will result. That is to say from the standpoint of chemical energy, the lower the atomic density and the greater the number of bonding defects at the habit plane, the more unstable the habit plane will be. Figure 4 showed the relationship of the precipitate morphology factor a/b and atomic plane density with atomic bonding ratio at the habit plane Z_i, but when it is considered that Z_S/Z_L in Equation (12) is equivalent to the atomic bonding ratio at the habit plane, the result of a greater tendency to granularity the lower the atomic density of a plane, that is to say the higher the atomic bonding ratio at the habit plane Z_i, may be considered to have been brought about by the magnitude of chemical interfacial energy.

Then again the elastic strain component of interfacial energy produced by misfit may be represented as [8]

$$\sigma_e = \mu a (1 + \phi - (1 + \phi^2)^{1/2}) /2\pi^2 \qquad (13)$$

where: ϕ is $2\pi\varepsilon / (1 - \nu)$; a is the lattice constant; ε is misfit strain; ν is Poisson's ratio; and μ is the shear modulus.

This shows that if the misfit is large interfacial energy increases, making for instability. Figure 3, however, showed no correlation between the degree of misfit and the morphology parameter, so that it can be inferred that its influence is less than that of chemical interfacial energy, and this has in part been experimentally verified [2].

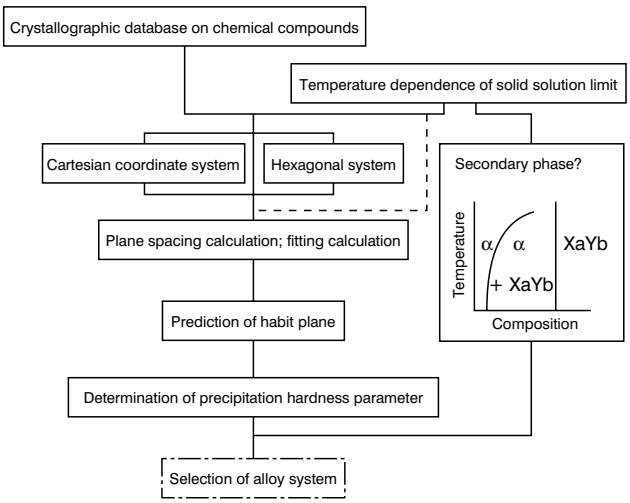

Figure 7 Flowchart showing design procedure for precipitation hardening copper alloys.

3.5 Methodology of Alloy Design Based on Crystallographic Structure of Precipitates

Figure 7 shows a flowchart summarizing the procedure for the design of copper alloys based on atomic alignment and solid mechanics. These are:

1) To extract from a database data and lattice constants pertaining to chemical compounds belonging the cubic, tetragonal, orthorhombic and hexagonal crystallographic systems, while excluding those compounds formed from elements for which there is no solid solution limit or solid-solution limit temperature dependence with reference to copper in the solid-state temperature range.
2) For each crystallographic system and based on the principles described in Section 2.1, to perform fitting calculations, select compounds that satisfy the conditions, and predict the habit plane, and when, in the above calculations, a plurality of habit planes are identified for the same compound, to narrow the focus based on the number of bonding defects as judged from the habit plane atomic density (atomic bonding ratio) at the habit plane.
3) To measure experimentally and estimate using

a calculation phase diagram the degree of precipitation δC of the selected compound at temperatures around 723~773K, and to estimate, using Equation (10) the precipitation hardening parameter $\partial\Delta\tau/\partial C$.

$$\partial\Delta\tau/\partial C \propto |\varepsilon|^{3/2} \cdot \delta C^{-1/2} \cdot Z_i^{1/2}/\sin\delta \qquad (14)$$

where: ε is the degree of lattice misfit; δC is the change in solute concentration in the matrix due to precipitation; θ is the angle formed by the habit plane and slip plane; and Z_i is the atomic bonding ratio

4) Since the relationship between an alloy content and the degree of precipitation strengthening can be estimated using precipitation hardening parameter $\partial\Delta\tau/\partial C$, the focus on alloy systems can be further narrowed, taking account of the amount of admixture in the alloy.
5) Finally, at the point at which the alloy system and the amount of alloy is designed, to verify by means of prototype production, and to design the manufacturing process.

In accordance with the alloy design process described above, it is necessary to know the temperature dependence of the solid-solution limit of the precipitate phase, and if a calculation phase diagram program [9] can be put into practice, the time required to narrow the focus to specific alloy systems will be significantly shortened. An approach to the structuring of a phase diagram by means of first principle calculations has also been made, and it is necessary to press forward with the creation of a more complete compound database, as well as the application of phase diagrams.

4. CONCLUSIONS

1) In crystallographic systems using Cartesian coordinates--cubic, tetragonal and orthorhombic, as well as in hexagonal systems, we selected alloy systems using Peason's Handbook on Crystallographic Data on chemical compounds, as a result of which we identified 101 cubic alloy systems, 16 tetragonal systems, 107 orthorhombic systems and 12 hexagonal systems.
2) We produced prototypes of some of the alloys selected, and for alloys that exhibited the property of precipitation hardening, we compared the results of orientation prediction and the results of observation by transmission electron microscope, and satisfactory agreement was obtained.
3) As a result of investigations of the relationship between precipitation hardenability $\partial\Delta\tau/\partial C$ and precipitate parameters, it was found that, more than the degree of lattice misfit or the angle the precipitate formed to the slip plane, influence was exerted by precipitate morphology, determined by the atomic plane density plane of the habit plane (atomic bonding ratio), and it was found that this could be expressed by

$$\partial\Delta\tau/\partial C \propto |\varepsilon|^{3/2} \cdot \delta C^{-1/2} \cdot Z_i^{1/2}/\sin\delta$$

where: ε is the degree of lattice misfit; δC is the change in solute concentration in the matrix due to precipitation; θ is the angle formed by the habit plane and slip plane; and Z_i is the atomic bonding ratio

4) From crystallographic data on the chemical compound forming the precipitate and data on the solid solution limit change for precipitate constituents, it becomes possible to narrow the focus to alloy systems capable of reaching high strength, and to predict the precipitation hardenability. By proceeding with calculations in accordance with the procedures presented in this paper and by some of the experiments, it is believed possible to design new high-strength alloys with far fewer process steps than with the conventional method.

REFERENCES

1) Japan Copper and Brass Association: Basis and Engineering Technology of Copper and Copper Alloys (Revised edition), 236. (in Japanese)
2) Fujiwara et al.: Transactions of Copper and Brass Workshop, 37, 106 (1998). (in Japanese)
3) V.Gerold and H.Haberkom: Phy. Status Solidi, 16, 675 (1966).
4) J.O.Linde: Ann. d. Phy., 15, 219 (1932).
5) P.Villars and L.D.Calvert: Peason's Handbook of Crystallographic Data, ASM, 1~4
6) P.Guyot: Phil. Mag., 24, 987 (1971).
7) I.S.Servi and D.Turnbull: Acta Met., 14, 161 (1966).
8) J.H.van der Merwe: J. Appl. Phys., 34, 117 (1963).
9) The Japan Institute of Metals: Basis and Application of Phase Diagram in Material Development and Design, 93 (1994). (in Japanese)